1521-0111/12/8205-803–813$25.00
MOLECULAR PHARMACOLOGY
Copyright © 2012 The American Society for Pharmacology and Experimental Therapeutics
Mol Pharmacol 82:803–813, 2012

Vol. 82, No. 5
79152/3799092

Molecular Mechanisms of Chloroquine Inhibition of Heterologously Expressed Kir6.2/SUR2A Channels

Daniela Ponce-Balbuena, Aldo A. Rodríguez-Menchaca, Angélica López-Izquierdo, Tania Ferrer, Harley T. Kurata, Colin G. Nichols, and José A. Sánchez-Chapula

"Unidad de Investigación Carlos Méndez" del Centro Universitario de Investigaciones Biomédicas de la Universidad de Colima, Colima, México (D.P.-B., A.L.-I., T.F., J.A.S.-C.); Departamento de Fisiología de la Facultad de Medicina de la Universidad Autónoma de San Luis Potosí, San Luis Potosí, México (A.A.R.-M.); Anesthesiology, Pharmacology, and Therapeutics, Faculty of Medicine, University of British Columbia, Vancouver, British Columbia, Canada (H.T.K.); and Cell Biology and Physiology, Center for the Investigation of Membrane Excitability Disorders, Washington University School of Medicine, St. Louis, Missouri (C.G.N.)

Received April 5, 2012; accepted July 31, 2012

ABSTRACT

Chloroquine and related compounds can inhibit inwardly rectifying potassium channels by multiple potential mechanisms, including pore block and allosteric effects on channel gating. Motivated by reports that chloroquine inhibition of cardiac ATP-sensitive inward rectifier K^+ current (I_{KATP}) is antifibrillatory in rabbit ventricle, we investigated the mechanism of chloroquine inhibition of ATP-sensitive potassium (K_{ATP}) channels (Kir6.2/SUR2A) expressed in human embryonic kidney 293 cells, using inside-out patch-clamp recordings. We found that chloroquine inhibits the Kir6.2/SUR2A channel by interacting with at least two different sites and by two mechanisms of action. A fast-onset effect is observed at depolarized membrane voltages and enhanced by the N160D mutation in the central cavity, probably reflecting direct channel block resulting from the drug entering the channel pore from the cytoplasmic side. Conversely, a slow-onset, voltage-independent inhibition of I_{KATP} is regulated by chloroquine interaction with a different site and probably involves disruption of interactions between Kir6.2/SUR2A and phosphatidylinositol 4,5-bisphosphate. Our findings reveal multiple mechanisms of K_{ATP} channel inhibition by chloroquine, highlighting the numerous convergent regulatory mechanisms of these ligand-dependent ion channels.

Introduction

ATP-sensitive potassium (K_{ATP}) channels couple cell metabolism to plasma membrane potassium fluxes in different cell types. K_{ATP} channels are hetero-octameric complexes comprising an inwardly rectifying K^+ channel, Kir6.x, and a regulatory sulfonylurea receptor SUR (Nichols, 2006; Hibino et al., 2010). Different combinations of these subunits generate unique K_{ATP} channel forms in a tissue-specific fashion, with Kir6.2 and SUR2A being major components of the cardiac K_{ATP} channel (Flagg and Nichols, 2011). The two subunits encode separable sensitivity to channel ligands: Kir6.2 is the principal site of ATP-induced channel inhibition and PIP_2-mediated activation, whereas SUR2A regulates MgADP activation. Two major classes of therapeutic compounds that target K_{ATP} channels are sulfonylureas and potassium channel openers. Both of these classes of compounds bind to SUR subunits. Other classes of compounds have been found to inhibit K_{ATP} channels by acting directly on Kir subunits; however, little is known about their mechanisms of action (Tamargo et al., 2004).

The antimalarial aminoquinolines mefloquine and chloroquine have been shown to inhibit Kir6.2/SUR1 channels during brief applications (~60 s). Mefloquine inhibited Kir6.2/SUR1 channels slightly more potently than chloroquine, with both compounds acting directly on the Kir6.2 subunit (Gribble et al., 2000). More recently, tamoxifen, mefloquine, and quinacrine have been demonstrated to inhibit Kir6.2/SUR2A channels by interfering with channel interactions with phosphatidylinositol 4,5-bisphosphate, a membrane phospholipid essential for channel function (López-Izquierdo

This work was supported by the National Institutes of Health National Heart, Lung, and Blood Institute [Grant R01 HL45742] (to C.G.N.); and Consejo Nacional de Ciencia y Tecnología–Secretaría de Educación Pública (México) [Grant CB-2008-01-105941] (to J.A.S.-C.). H.T.K. is supported by New Investigator awards from the Heart and Stroke Foundation of Canada and the Michael Smith Foundation for Health Research.

Article, publication date, and citation information can be found at http://molpharm.aspetjournals.org.

http://dx.doi.org/10.1124/mol.112.079152.

ABBREVIATIONS: K_{ATP}, ATP-sensitive potassium; SUR, sulfonylurea receptor; PIP_2, phosphatidylinositol 4,5-bisphosphate; I_{K1}, inward rectifier K+ current; I_{KATP}, ATP-sensitive inward rectifier K^+ current; I_{KACh}, K^+ current activated by muscarinic agonist; HEK, human embryonic kidney; WT, wild-type; CAD, cationic amphiphilic drug.

et al., 2010; Ponce-Balbuena et al., 2010). In addition, chloroquine inhibits the native cardiac inward rectifier currents, I_{K1}, I_{KATP} and I_{KACh} (Benavides-Haro and Sánchez-Chapula, 2000; Sánchez-Chapula et al., 2001; Noujaim et al., 2011). Chloroquine inhibits I_{K1} by interacting with two rings of negatively charged amino acids, formed by Glu224, Phe254, Asp255, Asp259, and Glu299 in the cytoplasmic pore of Kir2.1 (Rodríguez-Menchaca et al., 2008). The mechanisms of channel inhibition of I_{KATP} and I_{KACh} by chloroquine are not known.

Increasing inward rectifier currents (i.e., I_{K1}, I_{KATP}, or I_{KACh}) can shorten the action potential duration, potentially stabilizing and accelerating atrial and ventricular tachycardia and fibrillation (Noujaim et al., 2011), and some inherited mutations that increase I_{KATP} have been associated with early repolarization syndrome and idiopathic ventricular fibrillation (Haïssaguerre et al., 2009). During myocardial ischemia or hypoxia, I_{KATP} is activated, increasing the susceptibility of the heart to life-threatening ventricular tachyarrhythmias (Billman, 2008; Ehrlich, 2008). Recent studies suggested that blockade of inward rectifiers could, under certain conditions, offer a potentially useful antiarrhythmic strategy against ventricular and atrial tachyarrhythmias (Jost et al., 2004; Dhamoon and Jalife, 2005; Ehrlich, 2008).

Recent reports have also demonstrated that chloroquine could restore sinus rhythm after ventricular fibrillation induced by the potassium channel opener pinacidil (Noujaim et al., 2011). This effect was mediated by chloroquine inhibition of K_{ATP} channels. However, the mechanism of inhibition of the K_{ATP} channels is probably different from that of Kir2.1 channels. Kir6.2 lacks the negative charges corresponding to Kir2.1 residues Glu224 or Asp259. We suggest two alternative (although not mutually exclusive) mechanisms to explain the inhibition of Kir6.2 by chloroquine. First, chloroquine may block Kir6.2 channels via interaction with a binding site within the transmembrane vestibule. Second, chloroquine may act as a cationic amphiphilic drug and interfere with channel interactions with PIP_2, similar to the mechanism of action of tamoxifen, quinacrine, and mefloquine on I_{K1}, I_{KATP}, and I_{KACh} (Ponce-Balbuena et al., 2009, 2010; López-Izquierdo et al., 2010, 2011a). In this study, we have investigated these potential mechanisms of chloroquine action on Kir6.2/SUR2A. We report that both pore block and PIP_2 interference play a role in chloroquine inhibition of cardiac K_{ATP} currents.

Materials and Methods

DNA Constructs and Transfection of HEK293 Cells. Most Kir6.2 mutants were made with mouse Kir6.2 as a template in pcDNA3.1− (Invitrogen, Carlsbad, CA), using the QuikChange Site-Directed Mutagenesis Kit (Stratagene, La Jolla, CA). All mutations were confirmed by direct DNA sequencing. Kir6.2(C166S) cDNA in pcDNA3− was kindly donated by S. John, University of California in Los Angeles. The cDNAs encoding Kir6.2 wild-type (WT), SUR 2A, and Kir6.2 mutants were transiently transfected in HEK-293 cells with Lipofectamine 2000 reagent (Invitrogen) according to the manufacturer's instructions.

Patch-Clamp Recordings. Macropatch channel activity was recorded under an inside-out configuration of the patch-clamp technique (Hamill et al., 1981) using an Axopatch 200b amplifier (Molecular Devices, Sunnyvale, CA). Data acquisition and command potentials were controlled by pClamp 9.0 software (Molecular Devices). Patch pipettes with a resistance of 1 to 2 MΩ were made from borosilicate capillary glass (World Precision Instruments, Inc., Sarasota, FL). All the experiments were performed at 22°C, using a K^+-fluoride, K^+-vanadate, K^+-pyrophosphate, Mg^{+2}, and spermine-free solution (FVPP) to prevent current rundown (Huang et al., 1998) on both sides of the patch. The solution contained 123 mM KCl, 5 mM K_2EDTA, 7.2 mM K_2HPO_4, 8 mM KH_2PO_4, 0.1 mM Na_3VO_4, 5 mM KF, and 10 mM $K_4P_2O_7$, pH 7.2. The application of 30 mM K_2ATP was sufficient to abolish any detectable current through Kir6.2 and mutant channels, and off-line subtraction of currents recorded in 30 mM K_2ATP was used to subtract leak and endogenous currents.

Drugs. Chloroquine (Sigma-Aldrich, St. Louis, MO) was dissolved directly in the FVPP solution at the desired concentration. Inhibition of the current by pore blocking was measured 30 s after chloroquine bath application. To study the mechanism of inhibition of the current by interference between the interaction of the channel and PIP_2, the effects of chloroquine were measured 8 to 10 min after bath application in inside-out patches. L-α-Phosphatidylinositol-4,5-bisphosphate (Avanti Polar Lipids, Alabaster, AL) was stored as a 9.1 mM stock (in FVPP) and then dissolved to working concentrations in FVPP and sonicated for 30 min on ice before use.

Data Analysis. Patch-clamp data were processed using Clampfit 9.0 (Molecular Devices, Union City, CA) and analyzed in Origin 6.0 (OriginLab Corp., Northampton, MA). Data are presented as means ± S.E.M. In all experiments, n represents the number of cells. Student's t test was applied to compare individual data sets. A two-tailed probability value of less than 0.05 ($p = 0.05$) was considered statistically significant.

The fractional block of current (f) was plotted as a function of drug concentration ([D]) and the data were fit with a Hill equation (eq. 1):

$$f = 1/\{1/(1 + IC_{50}/[D]^h\} \quad (1)$$

to determine the half-maximal inhibitory concentration (IC_{50}) and the Hill coefficient h. The voltage dependence of block was measured by fitting fractional unblock as a function of voltage with a Woodhull equation (Woodhull, 1973) of the form (eq. 2):

$$I_{block}/I_{control} = 1/(1 + ([chloroquine]/K_d(0\ mV)e^{zFV/RT})) \quad (2)$$

where V is the test potential, K_d (0 mV) is the dissociation constant at 0 mV, z is the valence of block, F is the Faraday constant, R is the gas constant, and T is absolute temperature.

Results

Chloroquine Inhibits Kir6.2/SUR2A Currents by a Dual Mechanism. In Fig. 1A, we used excised inside-out patches expressing Kir6.2(WT)/SUR2A channels to characterize the inhibitory effects of 10 μM chloroquine applied to the intracellular side of the membrane. From a holding potential of −70 mV, test pulses to +50 mV followed by a hyperpolarization to −80 mV were applied every 15 s for 10 min. At +50 mV, chloroquine produced a fast time-dependent block within ~15 s of the initial drug application (54 ± 4%). With subsequent pulses to +50 mV, a further decrease in current amplitude progressed, reaching an apparent steady-state inhibition of 81 ± 3% (Fig. 1, A and D). Repolarization to −80 mV elicited a rapid component of blocker relief on short time scales. In addition, an immediate decrease of inward current amplitude (11 ± 2%) was observed in the first pulse in the presence of the drug, followed by a progressive decline in current amplitude, reaching an apparent steady-state inhibition of 46 ± 3% after 8 to 10 min (Fig. 1, A and D). The fast components of inhibition and relief may be due to pore block of the channel. The slow component of current inhibition observed at negative and positive membrane po-

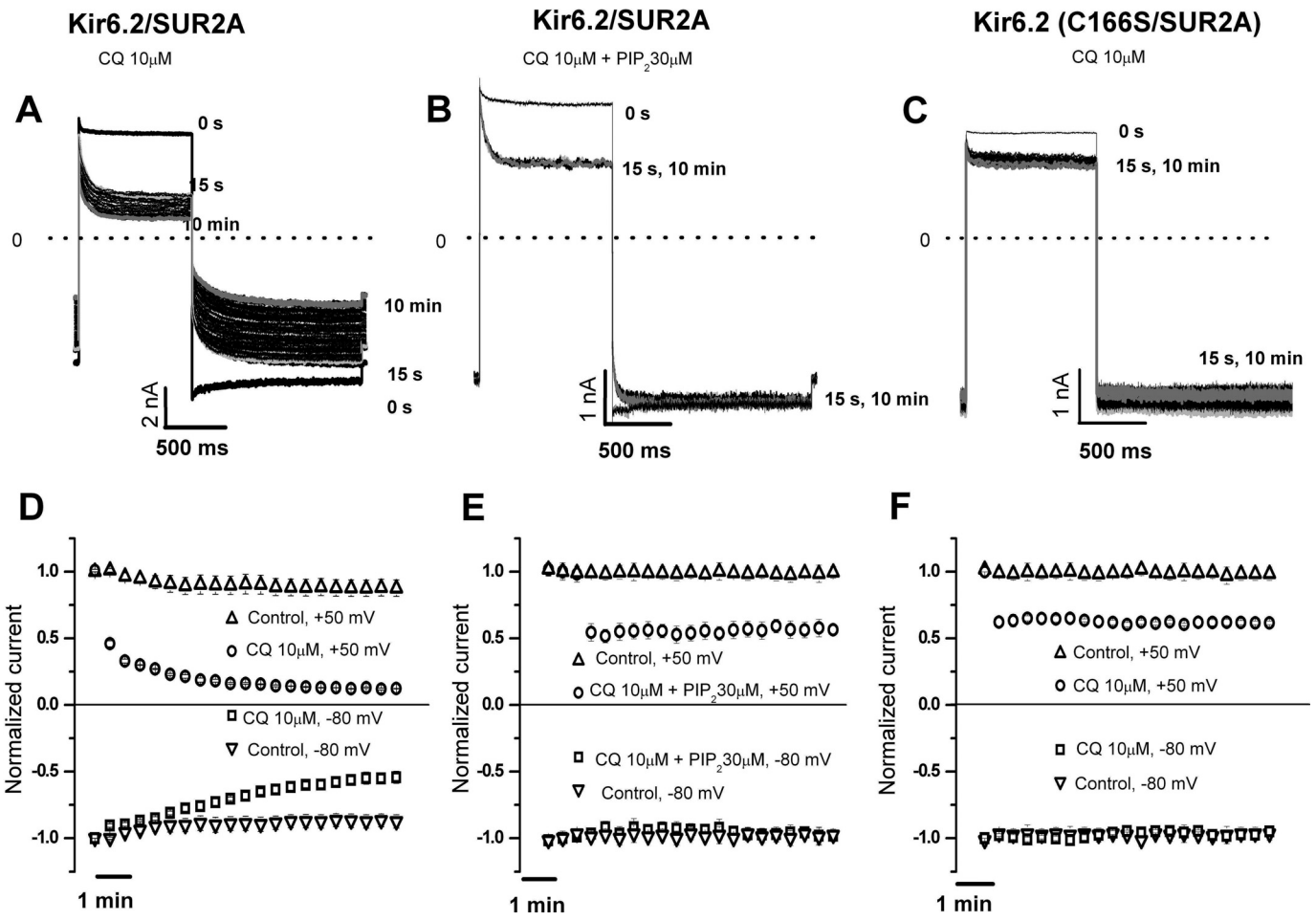

Fig. 1. Time-dependent inhibitory effect of chloroquine (CQ) on Kir6.2/SUR2A channels. Inside-out patches were pulsed from −70 mV to +50 mV and repolarized to −80 mV every 15 s, under control conditions and during a 10-min application of chloroquine. A to C, current traces under control conditions and in the presence of 10 μM chloroquine (after 15 s and 10 min of continuous application of the drug) are presented for (A) Kir6.2/SUR2A, (B) Kir6.2/SUR2A with 30 μM PIP_2, or (C) Kir6.2(C166S)/SUR2A. A includes current traces under control conditions (0 s) and the whole set of traces recorded in the presence of chloroquine. In B and C, for clarity, we only present the current traces obtained under control conditions and at 15 s and 10 min of application of the drug. The dashed line here and in all subsequent current traces indicates zero current. D to F, time course of the chloroquine inhibition in (D) Kir6.2/SUR2A, (E) Kir6.2/SUR2A with 30 μM PIP_2, and (F) Kir6.2(C166S)/SUR2A (means ± S.E.M of $n = 6$ experiments). Current amplitude changes during similar periods of time in the absence of chloroquine are included for comparison.

tentials may be due to disruption of channel-PIP_2 interactions by chloroquine. In the absence of chloroquine, current amplitude measured 10 min after patch excision was reduced significantly less (13 ± 2% at +50 mV and 12 ± 2% at −80 mV) (Fig. 1D).

To preserve Kir6.2 channel-PIP_2 interactions, we performed identical experiments on Kir6.2(WT)/SUR2A channels, in the presence of 30 μM exogenous PIP_2 (Fig. 1, B and E). Additional experiments were performed on the Kir6.2(C166S) mutant channel, which has a higher intrinsic open probability than WT Kir6.2 (Trapp et al., 1998) and is less prone to rundown arising from PIP_2 depletion than WT channels (Ribalet et al., 2006) (Fig. 1, C and F). In the presence of 30 μM exogenous PIP_2, chloroquine inhibited WT Kir6.2 with a fast time-dependent block (15 s after drug application), less pronounced (46 ± 4%) than that in PIP2-free solutions (54 ± 4%). No further current decrease was observed in the subsequent train of depolarizations (Fig. 1E). At −80 mV, chloroquine had no significant effect (Fig. 1E). In Kir6.2(C166S)/SUR2A channels, chloroquine produced only the fast component of block (presumed to be pore block) (Fig. 1, C and F). At +50 mV, chloroquine decreased current amplitude by only 39 ± 3%, less inhibition than was observed for Kir6.2(WT)/SUR2A (with or without exogenous PIP_2). This finding suggests that Kir6.2(C166S)/SUR2A channels are less sensitive than WT Kir6.2/SUR2A channels to the fast blocking effect observed at positive potentials. In similar experiments performed in the absence of chloroquine, current amplitudes did not significantly decrease after 10 min (Fig. 1, E and F).

The results described above suggest two different sites and mechanisms of Kir6.2 inhibition by chloroquine. The fast voltage-dependent effect observed at a positive voltage (+50 mV) may be induced by the drug entering the channel pore from the cytoplasmic surface. On the other hand, the slow voltage-independent inhibition of current, apparent at both +50 and −80 mV, probably results from disruption of Kir6.2 channel-PIP_2 interactions by chloroquine.

Effects of Chloroquine on Kir6.2/SUR2A Channel-PIP_2 Interaction. The Kir6.2 subunit has a low apparent affinity for PIP_2 (Ponce-Balbuena et al., 2010) relative to that of other Kir channels, and this property probably underlies a high sensitivity to inhibition by cationic amphiphilic drug (CADs) (Ponce-Balbuena et al., 2010; López-Izquierdo et al., 2011a). Kir6.2(C166S) increases the apparent PIP_2 affinity and renders

channels far less sensitive to rundown induced by PIP_2 depletion (Ribalet et al., 2006). Apparent PIP_2 affinity can also be weakened relative to that of WT channels with mutations such as R314A (Shyng et al., 2000). In Fig. 2, we examined the effects of chloroquine over this wide range of apparent affinity between the channel and PIP_2, using Kir6.2(WT)/SUR2A, Kir6.2(R314A)/SUR2A, and Kir6.2(C166S)/SUR2A channels. Currents recorded at −80 mV exhibit concentration-dependent inhibition by chloroquine. Figure 2D is a concentration-response curve of the inhibitory effects of chloroquine on WT Kir6.2/SUR2A channels, illustrating chloroquine inhibition of the channel with an IC_{50} of 19 μM. Figure 2E summarizes the concentration-dependent effects of chloroquine on the three channel isoforms studied. The strongest inhibition was observed in Kir6.2(R314A) channels, whereas the weakest inhibition was observed in Kir6.2(C166S). Overall, our results indicate that increased PIP_2 sensitivity results in weaker sensitivity to chloroquine. This trend holds true for both the "high PIP_2 sensitivity" Kir6.2(C166S) mutant, and the "low PIP_2 sensitivity" Kir6.2(R314A) mutant. These results strongly suggest that chloroquine reduces channel activity through a mechanism convergent with activation via the Kir6.2/SUR2A-PIP_2 interaction.

Chloroquine Pore Blocking Site Is within the Kir6.2 Central Vestibule. Chloroquine has been found to inhibit the strong inward rectifier Kir2.1 channel in a voltage-dependent manner; i.e., it produces stronger inhibition of outward than inward current. An alanine scan of Kir2.1 pore lining residues identified amino acids Glu224, Phe254, Asp259, and Glu299, located in the cytoplasmic pore region, as critical regulators of sensitivity to chloroquine block (Rodríguez-Menchaca et al., 2008). In contrast, the D172N mutation in the M2 transmembrane domain, important for strong polyamine-mediated inward rectification of Kir2.1, did not affect the chloroquine pore-blocking effects (Rodríguez-Menchaca et al., 2008). To probe the binding site for chloroquine within the Kir6.2 pore, we mutated multiple candidate residues in the pore-lining M2 helix and cytoplasmic domain and assessed the degree of chloroquine block. We restricted this scan to residues that project directly (except Cys166 and Glu288) into the ion-conducting pore (Kurata et al., 2004; Noujaim et al., 2010). We mutated multiple residues to Ala (V129A, T130A, L157A, N160A, L164A, C166S, F168A, and E288A) and uncharged residues to Asp and Glu (N160D, S212E, and S212E/N247D) (Fig. 3H). The pore-blocking effects of chloroquine were studied in excised inside-out patches in the continuous presence of 30 μM PIP_2 (to prevent PIP_2-mediated rundown, as in Fig. 1B). The effects of chloroquine on WT and different mutant channels are illustrated in Fig. 3. Block by 30 μM chloroquine was significantly reduced ($p < 0.05$) in L164A, C166A, and F168A mutant channels. In contrast, the N160D mutation in the central cavity significantly increased the chloroquine-blocking potency. However, introduction of charged residues in the cytoplasmic pore (S212E and S212E/N247D) did not modify the chloroquine potency. These results demonstrate that chloroquine block is more sensitive to mutations in the inner cavity than in the cytoplasmic vestibule, suggesting that the chloroquine binding site may be in the inner cavity formed by the transmembrane domains of the channel.

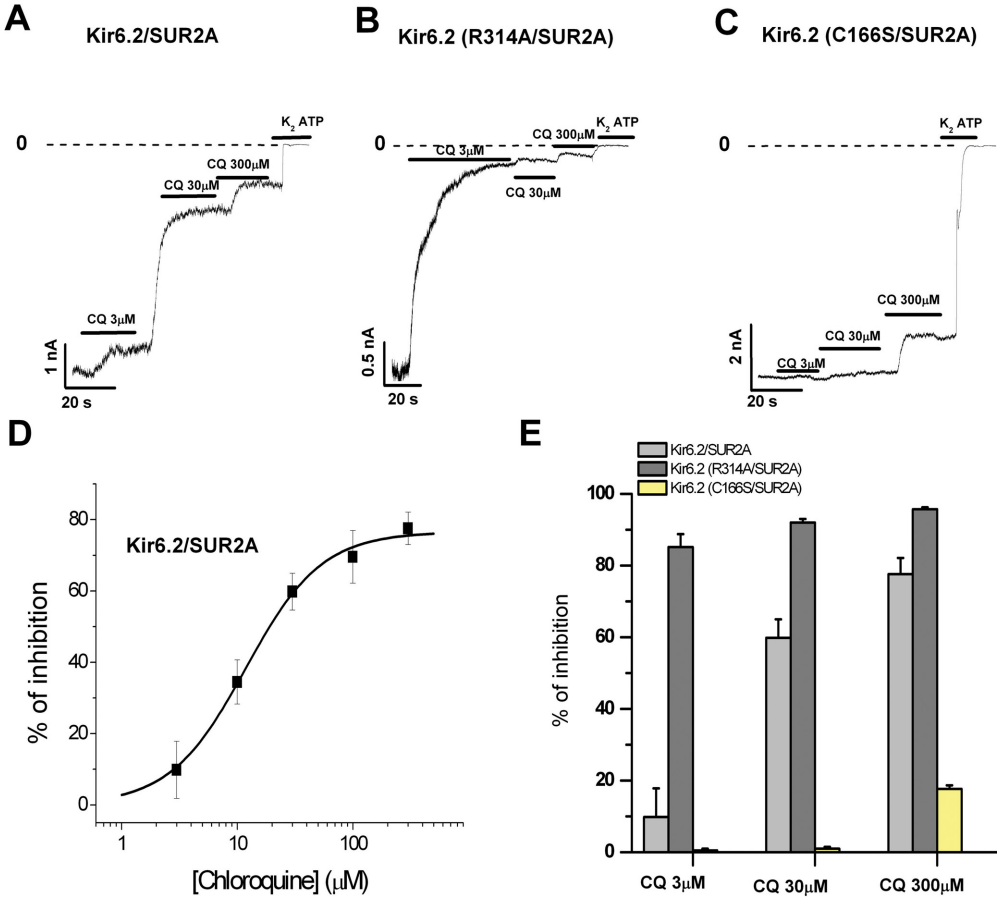

Fig. 2. Chloroquine (CQ) inhibits the Kir6.2 current, interfering with channel-PIP_2 interaction. A to C, macroscopic currents recorded at −80 mV from excised inside-out patches of HEK-293 cells expressing Kir6.2 and the mutants (R134A and C166S) + SUR2A in presence of different chloroquine concentrations as indicated. D, concentration-response curve of the effect of chloroquine on Kir6.2(WT)/SUR2A channel currents measured at −80 mV, similar to those shown in A. The IC_{50} of chloroquine was 11.8 ± 0.9 μM (n = 6 experiments at each concentration). E, summary of the inhibitory effects of chloroquine on the different channels (means ± S.E.M of n = 6 experiments at each concentration).

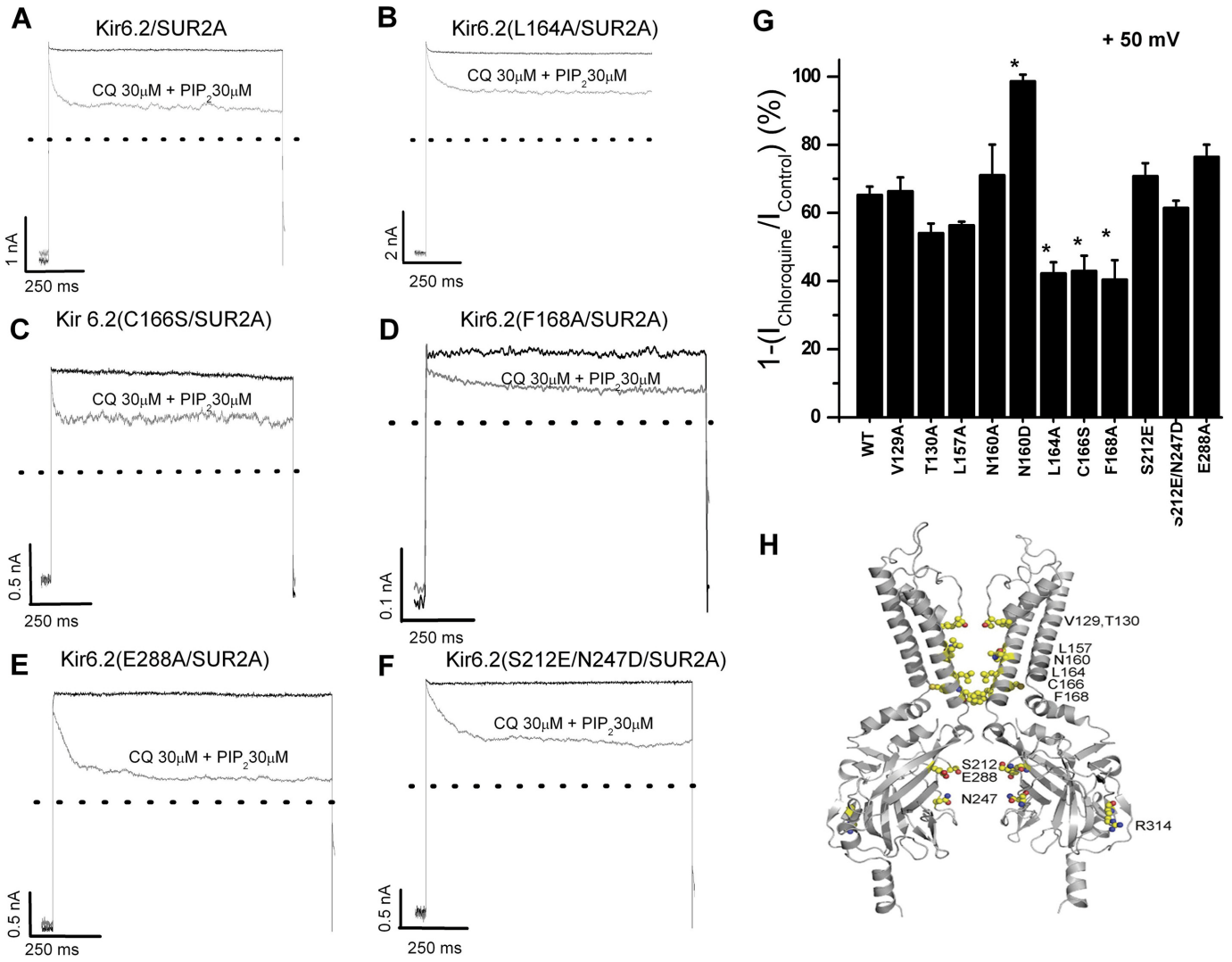

Fig. 3. Fast-onset chloroquine (CQ) blocking is altered by mutations in the central pore of Kir6.2. A to F, inside-out patch recordings illustrating the effects of 30 μM chloroquine in the continuous presence of 30 μM PIP_2 on WT and different Kir6.2 mutants (all coexpressed with SUR2A). From a holding potential (HP) of –70 mV, test pulses (TP) to +50 mV followed by a hyperpolarization to –70 mV were applied every 15 s for 10 min. G, percentage of current inhibition by 30 μM chloroquine plus 30 μM PIP_2 at +50 mV is shown (means ± S.E.M of $n = 5$ experiments). The bars represent steady-state inhibition of current by 30 μM chloroquine. H, molecular model of Kir6.2 constructed based on Kir2.2 (Protein Data Bank 3SPI), illustrating the position of mutations characterized in the study.

Characterization of the Pore-Blocking Effect of Chloroquine on Kir6.2/SUR2A and Kir6.2(N160D)/SUR2A Channels. To characterize the pore-blocking effects of chloroquine on Kir6.2/SUR2A and Kir6.2(N160D)/SUR2A channels, we used excised inside-out patches, in the continuous presence of 30 μM PIP_2. In Fig. 4, patches were held at −90 mV and pulsed between −90 and +70 mV under control conditions and in the presence of 10 μM chloroquine. Under control conditions in the absence of Mg^{2+} and polyamines, no inward rectification is observed. In the presence of chloroquine, concentration- and voltage-dependent inward rectification was induced. Current-voltage (I-V) relationships (Fig. 4B), measured at the end of each pulse, depict the effects of 0, 10, 30, and 100 μM chloroquine. Concentration-response curves of the blocking effect of chloroquine on Kir6.2/SUR2A at 10, 30, and 50 mV are shown in Fig. 4C. We fitted the data with eq. 1, assuming 1:1 stoichiometry between the drug and the channel, to generate steady-state apparent equilibrium dissociation constants for chloroquine (appK_d). Figure 4D illustrates the relative conductance-voltage relationships obtained for chloroquine block of Kir6.2/SUR2A currents ($I_{chloroquine}/I_{control}$). The continuous lines are fits of the Woodhull equation, yielding an apparent K_d (0 mV) = 2.1×10^{-4} M^{-1} and an estimated voltage dependence $z = 1.1 \pm 0.12$ ($n = 6$).

Cardiac (Kir6.2/SUR2A) and pancreatic (Kir6.2/SUR1) K_{ATP} channels do not show strong inward rectification (Ashcroft, 1988; Nichols and Lederer, 1991). This is attributed to the fact that WT Kir6.2 contains no negative charges in M2 and is also missing important charged residues found in the cytoplasmic pore of Kir2.1, such as Glu224 (Kir6.2 residue Ser212) and Asp259 (Kir6.2 residue Asn247). However, introduction of a negative charge (Asp or Glu) at Kir6.2 position Asn160 (equivalent to the "rectification controller" residue 172 in the classic strong inward rectifier Kir2.1) results in channels that rectify just as strongly as Kir2.1 (Shyng et al., 1997; Kurata et al., 2004). In the present work, we also characterized the blocking effects of chloroquine on Kir6.2(N160D)/SUR2A mutants (Fig. 5A). Raw currents (Fig.

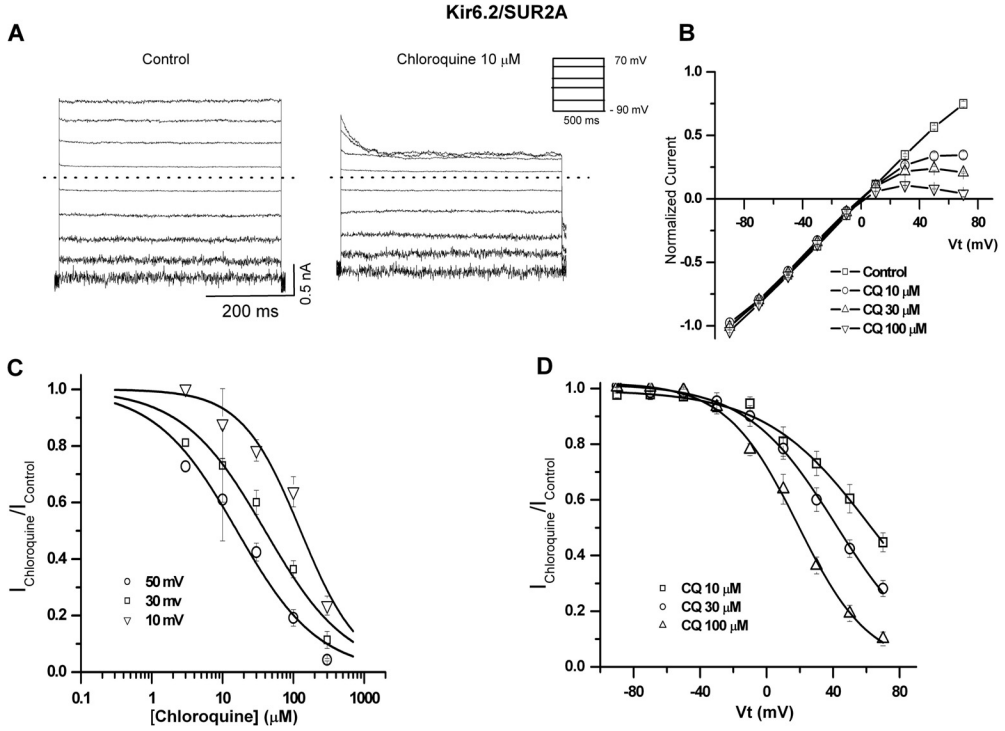

Fig. 4. Voltage- and concentration-dependent pore-blocking effect of chloroquine (CQ) on Kir6.2/SUR2A channels. A, representative Kir6.2/SUR2A current elicited in excised inside-out patches in the absence (control) and presence of 10 μM chloroquine. B, steady-state current-voltage relationships under control conditions and in various chloroquine concentrations. C, residual unblocked current is plotted against chloroquine concentration for three representative voltages, fitted with the Hill equation at each voltage. D, residual unblocked current is plotted against membrane voltage and fitted with the Woodhull equation. All experiments were performed with 30 μM PIP_2.

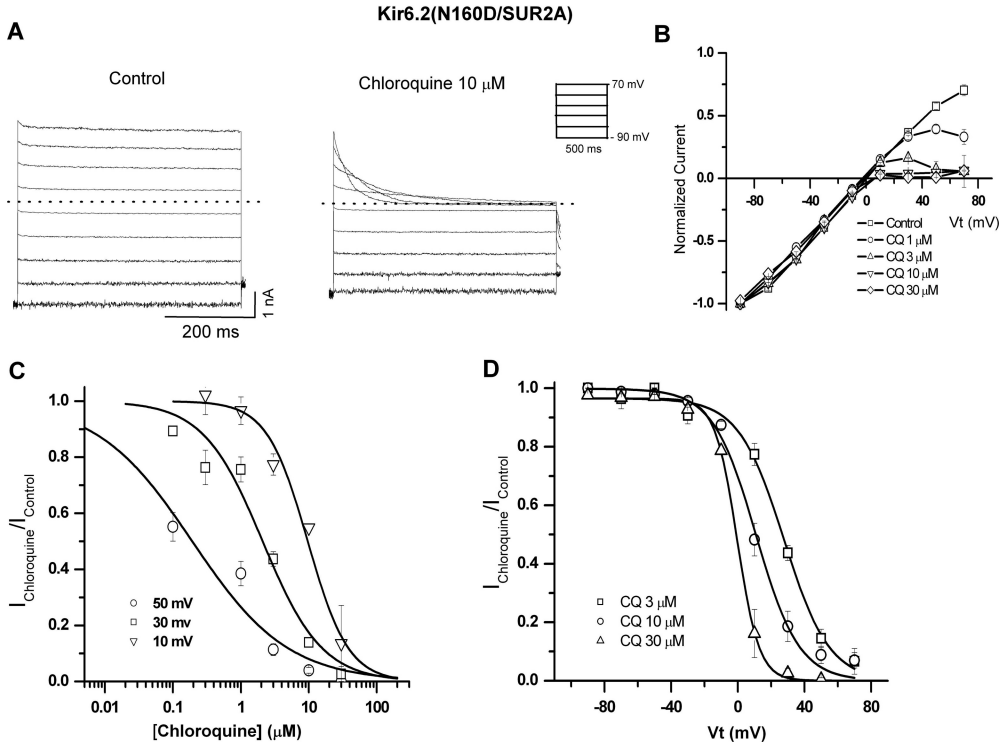

Fig. 5. Inhibition of Kir6.2(N160D)/SUR2A channels by intracellular chloroquine (CQ). A, representative Kir6.2(N160D)/SUR2A current recorded in excised inside-out patches in the absence (control) and presence of 10 μM chloroquine. B, steady-state I-V curves in the absence and presence of chloroquine at the indicated concentrations. C, concentration-response curves for chloroquine effects at different voltages, each fitted with the Hill equation. D, voltage dependence of intracellular chloroquine block, fitted with the Woodhull equation. All experiments were performed in the continuous presence of 30 μM PIP_2.

5A) and steady-state current-voltage (I-V) relationships (Fig. 5B) illustrate that chloroquine inhibits Kir6.2(N160D)/SUR2A channels more potently than WT Kir6.2. Similar to WT Kir6.2 channels (Fig. 4), we fitted concentration-response curves (Fig. 4C) to obtain apparent equilibrium dissociation constants for chloroquine. We also derived an estimated apparent K_d (0 mV) of 2.1×10^{-5} M^{-1} and effective valence of chloroquine block $z = 2.4 \pm 0.3$ (Fig. 5D). Chloroquine block of Kir6.2(N160D) was more potent and steeply voltage-dependent than that of WT Kir6.2 channels.

We studied the kinetics of chloroquine block of Kir6.2(WT)/SUR2A and Kir6.2(N160D)/SUR2A channels with voltage steps to potentials between +10 and +70 mV at different chloroquine concentrations, similar to records shown in Figs. 4A and 5A. Current relaxation arising from chloroquine block was fitted with a single exponential function (the first 3 ms of current traces were omitted to avoid errors arising from inadequate voltage clamp). To analyze the concentration dependence of the rate of inhibition, we plotted the reciprocal of the time constants for channel block

($1/\tau_{on}$) against chloroquine concentration at multiple voltages for Kir6.2/SUR2A and Kir6.2(N160D) (Fig. 6, A and B). We fit the data to eq. 3:

$$1/\tau_{on} = k_{on} \cdot [\text{chloroquine}] + k_{off} \quad (3)$$

From the slope of the linear fit for each voltage, we obtained apparent second-order rate constants (k_{on}) for channel block. There was no significant difference between k_{on} for WT and N160D mutant Kir6.2/SUR2A channels. To determine the voltage dependence of k_{on}, we plotted ln k_{on} against membrane voltage (Fig. 6D). In Fig. 6C, appK_d values obtained from concentration-response curves (Figs. 4C and 5C) at different membrane potentials are plotted, illustrating the greater chloroquine potency on Kir6.2(N160D) channels relative to that on WT Kir6.2. Using experimentally determined K_d (Fig. 6C) and k_{on} values (Fig. 6D), we calculated k_{off} as a function of membrane potential (Fig. 6E). This derivation implies a significant slowing of k_{off} in Kir6.2(N160D)/SUR2A channels relative to WT Kir6.2.

Chloroquine Unblock from Kir6.2/SUR2A and Kir6.2(N160D)/SUR2A Channels. Unblocking kinetics were inferred from the time course of repolarization-induced recovery of current at different hyperpolarizing membrane potentials. Kir6.2(WT)/SUR2A (Fig. 7A) or Kir6.2(N160D)/SUR2A (Fig. 7B) channels were blocked with depolarizing pulses to +50 mV followed by hyperpolarizing steps to −30, −50, −70, and −90 mV, in the presence of chloroquine. The unblocking time courses were fit with sums of three exponential components. All components of the unblocking time had similar voltage dependence in both channels (Fig. 7C), although the relative contribution of the slowest time constant ($\tau 3$) was significantly larger in Kir6.2(N160D) channels (Fig. 7D). Overall, the predominant effect of the Kir6.2(N160D) mutation was on blocker unbinding kinetics, although the process cannot be simply described by a single-step blocking model.

We further characterized chloroquine unblock at different drug concentrations. Figure 8, A to D, shows examples of currents recorded in 0.3 to 100 μM chloroquine, with blockade elicited by depolarizing pulses to +70 mV, followed by unblock at −70 mV. In Fig. 8E, we measured the half-time of block recovery ($t_{1/2}$) as a function of chloroquine concentration. These results illustrate that recovery from block is dependent on chloroquine concentration, with high drug con-

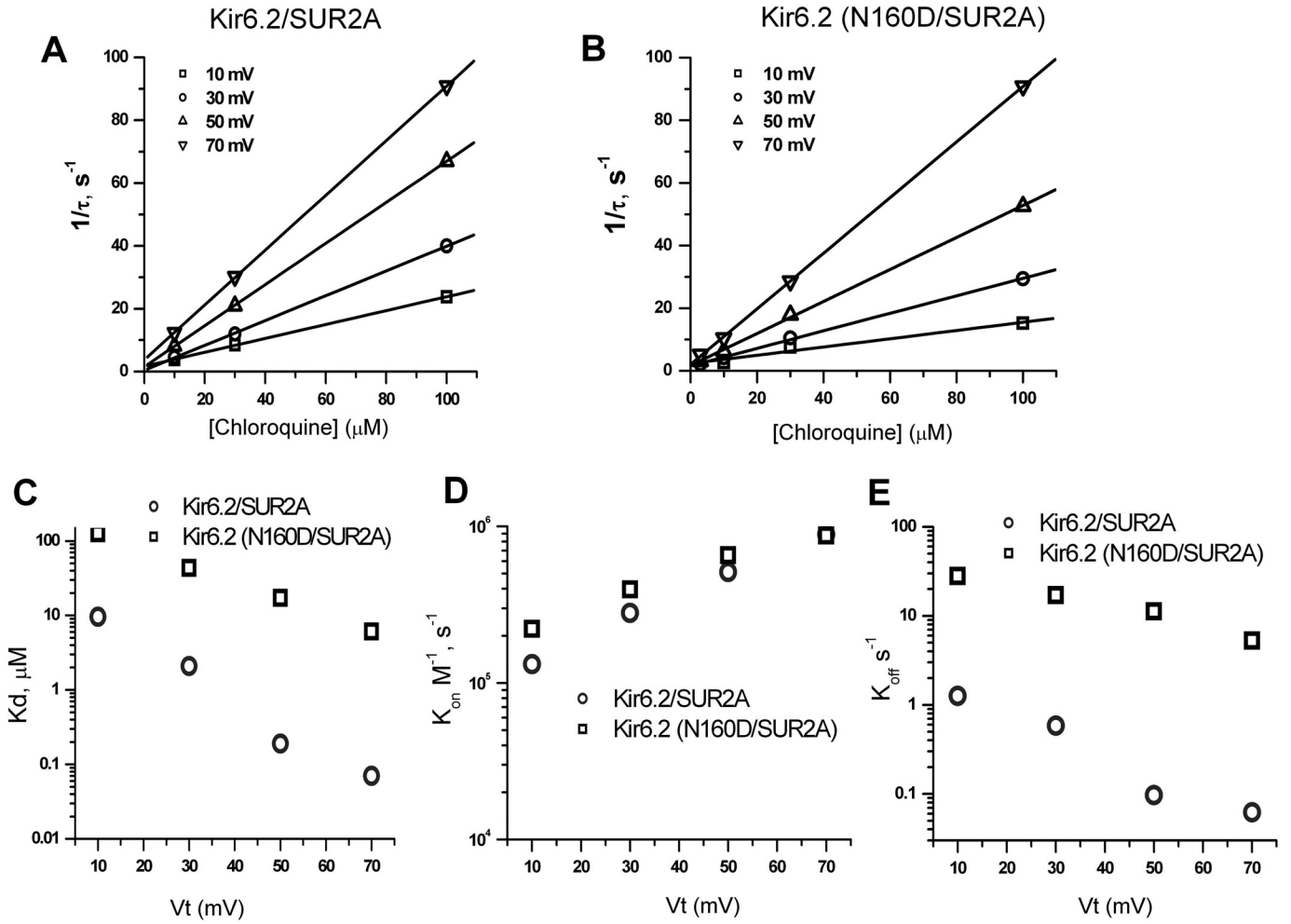

Fig. 6. Kinetic analysis of Kir6.2/SUR2A and Kir6.2 (N160D)/SUR2A blockade by chloroquine. A and B, reciprocals of the time constants ($1/\tau$) obtained from exponential fits of chloroquine-dependent current relaxation (Figs. 4A and 5A) are plotted against chloroquine concentration at various voltages. Solid lines are linear fits to data. C, K_d values obtained from concentration-dependent inhibition of steady-state currents at different membrane potentials. D, voltage dependence of blocking rate constants (k_{on}). E, voltage dependence of the unblocking rate constant (k_{off}). Data points were obtained by multiplying K_d by k_{on} for each voltage.

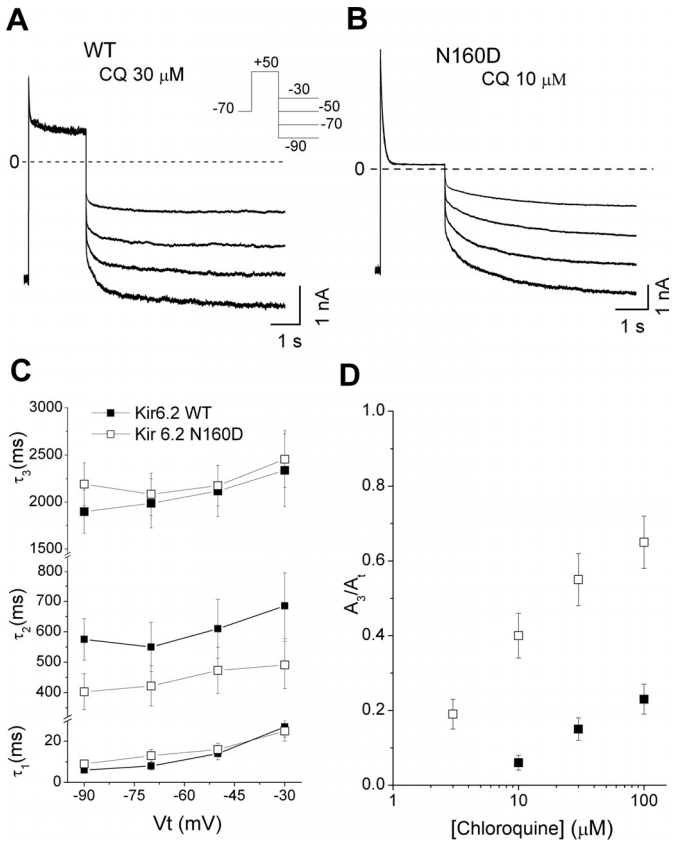

Fig. 7. Chloroquine (CQ) unblock of Kir6.2/SUR2A and Kir6.2 (N160D)/SUR2A channels. A and B, current traces from Kir6.2 and Kir6.2(N160D)-containing channels were elicited by a depolarizing voltage step to +50 mV and then repolarizing the membrane to different voltages. C, unblocking time constants were fit with a sum of three exponentials, with time constants plotted as a function of hyperpolarizing test voltage. D, relative amplitude of the component 3 (A_3/A_t) as a function of chloroquine concentration.

centrations increasing the contribution of the slower (A_3) component.

Spermine Block Protects Kir6.2(N160D)/SUR2A Channels from Chloroquine Block. Data presented thus far suggest that the chloroquine-binding site responsible for fast voltage-dependent block of Kir6.2(N160D) and WT Kir6.2 channels is located within the central cavity. We tested whether prior binding of spermine to Kir6.2(N160D) channels might protect them from chloroquine block. To address this question, we applied repetitive depolarizing pulses to +50 mV, followed by repolarization to −80 mV (Fig. 9). Application of 10 μM spermine during the depolarizing pulse elicited blockade of the outward current, followed by fast recovery from block when the membrane voltage was repolarized to −80 mV (Fig. 9). In a second trial, 10 μM chloroquine was applied in place of spermine, causing almost complete blockade of the outward current, followed by slow recovery from block at −80 mV. Finally, in a third trial performed on the same patch, 10 μM spermine was first applied alone for 3 s, followed by application of 10 μM spermine together with 10 μM chloroquine. Spermine alone was sufficient to induce complete blockade of outward current, so coapplication of spermine plus chloroquine did not cause any additional change in the outward current. However, upon repolarization, most of the recovery from block was rapid, similar to that observed when spermine was applied alone, and only approximately 10% of the recovery process followed a slow time course (Fig. 9). These results suggest that spermine occludes chloroquine binding in Kir6.2(N160D)/SUR2A channels, indicating that spermine and chloroquine share a similar binding site in the inner cavity.

Discussion

In human and animal models, inward rectifier potassium channels have been implicated in the perpetuation of reentrant tachyarrhythmias in the normal and diseased heart. Under certain conditions, blockade of inward rectifiers could offer a useful strategy against ventricular and atrial tachyarrhythmias (Varró et al., 2004; Dhamoon and Jalife, 2005; Ehrlich, 2008). It is well known that activation of I_{KATP} shortens the cardiac action potential duration in response to metabolic stresses such as ischemia, increasing the susceptibility of the heart to life-threatening ventricular tachyarrhythmias (Billman, 2008; Ehrlich, 2008). One possible mechanism underlying this observation is the contribution of I_{KATP} to left ventricular-right ventricular heterogeneity in the anterior epicardial action potential duration during global ischemia, related in part to the higher density of I_{KATP}, resulting from higher Kir6.1/Kir6.2 mRNA levels in the left ventricle than in the right ventricle (Pandit et al., 2011).

A recent study demonstrated that chloroquine inhibition of three different Kir channel currents (I_{K1}, I_{KACh}, and I_{KATP}) is antifibrillatory in atria and ventricles (Noujaim et al., 2010). In their study, chloroquine reduced fibrillatory frequency (atrial or ventricular), and effectively terminated arrhythmias, leading to resumption of sinus rhythm. In cardiac myocytes, chloroquine inhibits I_{K1}, I_{KACh}, and I_{KATP} with a similar potency (Noujaim et al., 2010), but at negative membrane potentials the effect on I_{K1} is smaller than the effect on I_{KATP}. Comparative molecular modeling and ligand docking of chloroquine in the intracellular domains of Kir2.1 suggested that chloroquine interacts with negatively charged amino acids facing the cytoplasmic pore of the channel (Rodríguez-Menchaca et al., 2008; Noujaim et al., 2010). In contrast, chloroquine was predicted to bind the Kir6.2 cytoplasmic pore in a configuration that seemed unlikely to impede potassium ion permeation (Noujaim et al., 2010).

Our findings suggest that chloroquine inhibits the Kir6.2/SUR2A channel by interaction with at least two different sites and by two mechanisms of action. A fast voltage-dependent, pore-blocking effect observed at positive voltages is enhanced by the N160D mutation and reflects block within the permeation pathway resulting from the drug entering the channel pore from the cytoplasmic side. On the other hand, the slow-onset, voltage-independent inhibition of the current produced by the drug is induced at a different site and probably mediated by disruption of the Kir6.2/SUR2A-PIP_2 interaction.

Activation by membrane PIP_2 is a common feature of all Kir channels. The direct interaction between negative phosphate head groups of PIP_2 and positively charged residues in N and C termini is essential for activation of channels (Fan and Makielski, 1997; Lopes et al., 2002; Schulze et al., 2003; Hansen et al., 2011). CADs such as chloroquine comprise a hydrophilic cationic side chain and apolar ring systems within one molecule (Allan and Michell, 1975). Intercalated in a bilayer, the cationic group is arranged between the

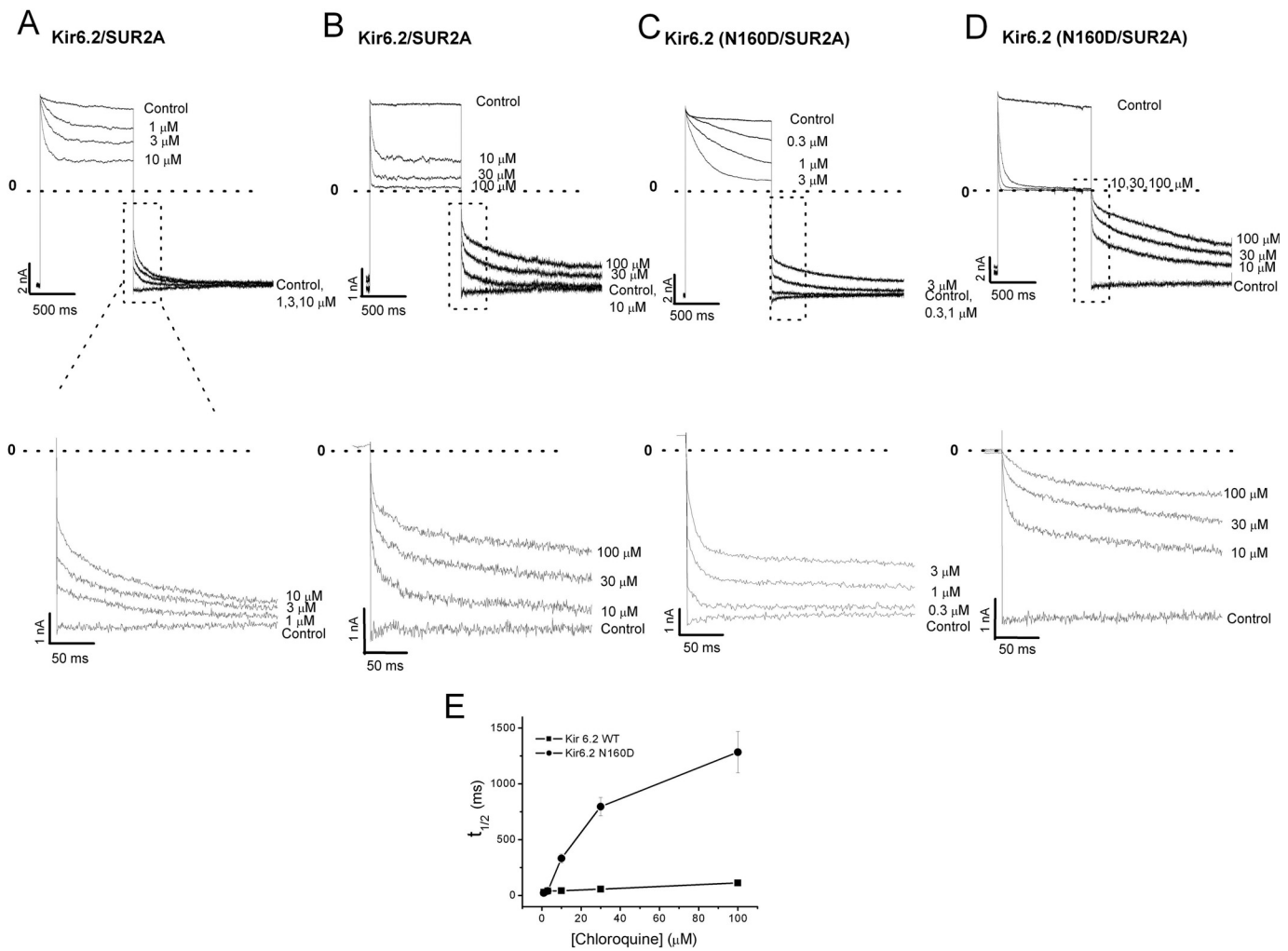

Fig. 8. Chloroquine unblock depends on drug concentration. A to D, top panels, currents were elicited in various chloroquine concentrations by blocking at +70 mV and unblocking at −70 mV Kir6.2/SUR2A, and Kir6.2(N160D)/SUR2A, as indicated. Bottom panels, the first 250 ms of the chloroquine unblock time course are displayed. E, concentration dependence of the half-time ($t_{1/2}$) needed for chloroquine unblock.

hydrophilic head groups, whereas the hydrophobic portion of the CAD is positioned between the fatty acid tails (Seeman, 1972; Conrad and Singer, 1981). This arrangement may directly affect PIP_2 interactions with ion channels. Consistent with this observation, channels relatively resistant to rundown mediated by PIP_2 depletion such as Kir2.1 ("high PIP_2 affinity") are less sensitive to CADs such as bupivacaine, mepyramine, tamoxifen, mefloquine, carvedilol, and quinacrine (Zhou et al., 2001; Liu et al., 2007; Ponce-Balbuena et al., 2009, 2010; Ferrer et al., 2011; López-Izquierdo et al., 2011a,b). Channels with weak PIP_2 interactions (e.g., Kir2.3 and Kir6.2) are highly sensitive to these drugs. The order of reported channel sensitivity to CADs is Kir3.1/3.4 > Kir6.2 > Kir2.3 > Kir2.1 (Ponce-Balbuena et al., 2009, 2010; Ferrer et al., 2011; López-Izquierdo et al., 2011a,b). Recently, we found that quinacrine induced a double action toward Kir channels, i.e., direct pore block of Kir2.1 and Kir2.3 and interference in PIP_2-Kir channel interaction in a differential manner, Kir6.2 ~ Kir2.3 > Kir2.1 (López-Izquierdo et al., 2011a).

In this study we have presented evidence that chloroquine may interfere with the Kir6.2-PIP_2 interaction. In particular, our observation that Kir6.2(C166S)/SUR2A channels were less sensitive to chloroquine and Kir6.2(R314A)/SUR2A were more sensitive was consistent with the effects of these mutations on channel sensitivity to PIP_2 (Shyng et al., 2000; Ribalet et al., 2006). In addition, coapplication of chloroquine with exogenous PIP_2 prevented the slow component of chloroquine-mediated current inhibition (Fig. 1B).

Alanine scans of pore-lining residues identified amino acids located in the Kir6.2 subunit central cavity region as critical in chloroquine-mediated block (Leu164, Cys166, and Phe168). Mutations L164A, C166A, and F168A significantly reduced the chloroquine blocking potency, suggesting their participation in the chloroquine-binding site. However, in crystal structures of eukaryotic Kir channels (Hansen et al., 2011; Whorton and MacKinnon, 2011), residues equivalent to Cys166 do not face the pore. Therefore, the mutation may be inducing an indirect perturbation of the chloroquine-binding site. The Kir6.2(N160D)/SUR2A mutant channel shows strong polyamine-mediated inward rectification (Shyng et al., 1997). The potency of block by chloroquine was also significantly increased in N160D mutant channels, consistent with the drug-binding site being in the central cavity, a conclusion that is reinforced by the demonstration that spermine occupancy can occlude chloroquine from its binding site.

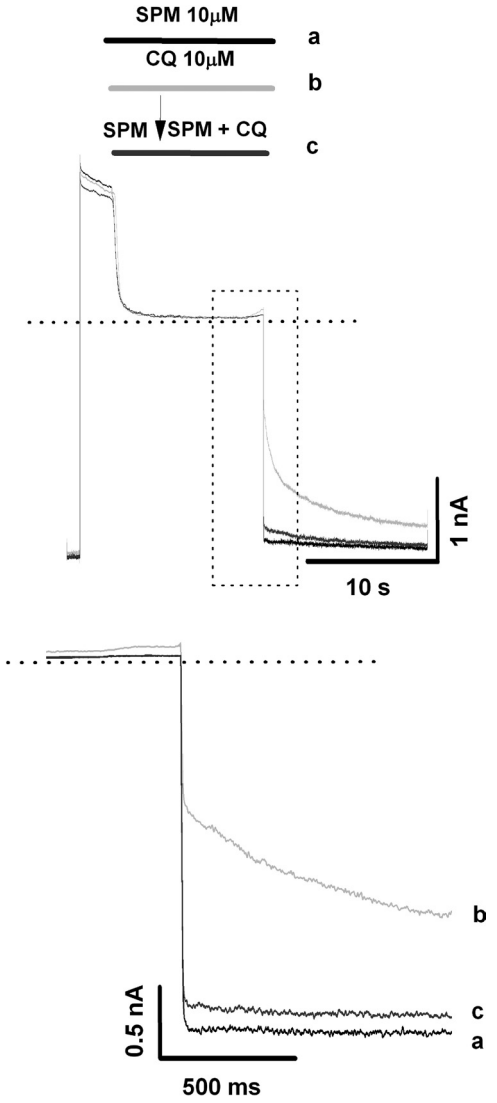

Fig. 9. Spermine (SPM) partially protects Kir6.2 (N160D)/SUR2A mutant channels from chloroquine (CQ) block. Top panel, patches were depolarized to +50 mV for 14 s, followed by repolarization to −80 mV. During the first trial, 10 μM spermine was applied alone during the depolarizing pulse. The experiment was repeated with 10 μM chloroquine application. In a third trial performed on the same patch, 10 μM spermine was first applied alone for 3 s, followed by application of 10 μM spermine together with 10 μM chloroquine. Bottom panel, the first second of repolarization-induced recovery of current at −80 mV is highlighted and depicts all three experimental treatments. a, recovery of spermine alone block by repolarization. b, recovery of chloroquine alone block by repolarization. c, recovery of spermine and spermine + chloroquine block by repolarization.

Acknowledgments

We thank Miguel A. Flores for technical assistance.

Authorship Contributions

Participated in research design: Kurata, Nichols, and Sánchez-Chapula.

Conducted experiments: Ponce-Balbuena, Rodríguez-Menchaca, López-Izquierdo, and Ferrer.

Performed data analysis: Ponce-Balbuena, Rodríguez-Menchaca, López-Izquierdo, and Ferrer.

Wrote or contributed to the writing of the manuscript: Ponce-Balbuena, Ferrer, Kurata, Nichols, and Sánchez-Chapula.

References

Allan D and Michell RH (1975) Enhanced synthesis de novo of phosphatidylinositol in lymphocytes treated with cationic amphiphilic drugs. *Biochem J* **148:**471–478.
Ashcroft FM (1988) Adenosine 5′-triphosphate-sensitive potassium channels. *Annu Rev Neurosci* **11:**97–118.
Benavides-Haro DE and Sánchez-Chapula JA (2000) Chloroquine blocks the background potassium current in guinea pig atrial myocytes. *Naunyn Schmiedebergs Arch Pharmacol* **361:**311–318.
Billman GE (2008) The cardiac sarcolemmal ATP-sensitive potassium channel as a novel target for anti-arrhythmic therapy. *Pharmacol Ther* **120:**54–70.
Conrad MJ and Singer SJ (1981) The solubility of amphipathic molecules in biological membranes and lipid bilayers and its implications for membrane structure. *Biochemistry* **20:**808–818.
Dhamoon AS and Jalife J (2005) The inward rectifier current (IK1) controls cardiac excitability and is involved in arrhythmogenesis. *Heart Rhythm* **2:**316–324.
Ehrlich JR (2008) Inward rectifier potassium currents as a target for atrial fibrillation therapy. *J Cardiovasc Pharmacol* **52:**129–135.
Fan Z and Makielski JC (1997) Anionic phospholipids activate ATP-sensitive potassium channels. *J Biol Chem* **272:**5388–5395.
Ferrer T, Ponce-Balbuena D, López-Izquierdo A, Aréchiga-Figueroa IA, de Boer TP, van der Heyden MA, and Sánchez-Chapula JA (2011) Carvedilol inhibits Kir2.3 channels by interference with PIP_2-channel interaction. *Eur J Pharmacol* **668:**72–77.
Flagg TP and Nichols CG (2011) "Cardiac KATP": a family of ion channels. *Circ Arrhythm Electrophysiol* **4:**796–798.
Gribble FM, Davis TM, Higham CE, Clark A, and Ashcroft FM (2000) The antimalarial agent mefloquine inhibits ATP-sensitive K-channels. *Br J Pharmacol* **131:**756–760.
Haïssaguerre M, Chatel S, Sacher F, Weerasooriya R, Probst V, Loussouarn G, Horlitz M, Liersch R, Schulze-Bahr E, Wilde A, et al. (2009) Ventricular fibrillation with prominent early repolarization associated with a rare variant of KCNJ8/KATP channel. *J Cardiovasc Electrophysiol* **20:**93–98.
Hamill OP, Marty A, Neher E, Sakmann B, and Sigworth FJ (1981) Improved patch-clamp techniques for high-resolution current recording from cells and cell-free membrane patches. *Pflugers Arch* **391:**85–100.
Hansen SB, Tao X, and MacKinnon R (2011) Structural basis of PIP2 activation of the classical inward rectifier K^+ channel Kir2.2. *Nature* **477:**495–498.
Hibino H, Inanobe A, Furutani K, Murakami S, Findlay I, and Kurachi Y (2010) Inwardly rectifying potassium channels: their structure, function, and physiological roles. *Physiol Rev* **90:**291–366.
Huang CL, Feng S, and Hilgemann DW (1998) Direct activation of inward rectifier potassium channels by PIP2 and its stabilization by G$\beta\gamma$. *Nature* **391:**803–806.
Jost N, Virág L, Hála O, Varró A, Thormählen D, and Papp JG (2004) Effect of the antifibrillatory compound tedisamil (KC-8857) on transmembrane currents in mammalian ventricular myocytes. *Curr Med Chem* **11:**3219–3228.
Kurata HT, Phillips LR, Rose T, Loussouarn G, Herlitze S, Fritzenschaft H, Enkvetchakul D, Nichols CG, and Baukrowitz T (2004) Molecular basis of inward rectification: polyamine interaction sites located by combined channel and ligand mutagenesis. *J Gen Physiol* **124:**541–554.
Liu B, Jia Z, Geng X, Bei J, Zhao Z, Jia Q, and Zhang H (2007) Selective inhibition of Kir currents by antihistamines. *Eur J Pharmacol* **558:**21–26.
Lopes CM, Zhang H, Rohacs T, Jin T, Yang J, and Logothetis DE (2002) Alterations in conserved Kir channel-PIP2 interactions underlie channelopathies. *Neuron* **34:**933–944.
López-Izquierdo A, Aréchiga-Figueroa IA, Moreno-Galindo EG, Ponce-Balbuena D, Rodríguez-Martínez M, Ferrer-Villada T, Rodríguez-Menchaca AA, van der Heyden MA, and Sánchez-Chapula JA (2011a) Mechanisms for Kir channel inhibition by quinacrine: acute pore block of Kir2.x channels and interference in PIP2 interaction with Kir2.x and Kir6.2 channels. *Pflugers Arch* **462:**505–517.
López-Izquierdo A, Ponce-Balbuena D, Ferrer T, Rodríguez-Menchaca AA, and Sánchez-Chapula JA (2010) Thiopental inhibits function of different inward rectifying potassium channel isoforms by a similar mechanism. *Eur J Pharmacol* **638:**33–41.
López-Izquierdo A, Ponce-Balbuena D, Moreno-Galindo EG, Aréchiga-Figueroa IA, Rodríguez-Martínez M, Ferrer T, Rodríguez-Menchaca AA, and Sánchez-Chapula JA (2011b) The antimalarial drug mefloquine inhibits cardiac inward rectifier K^+ channels: evidence for interference in PIP2-channel interaction. *J Cardiovasc Pharmacol* **57:**407–415.
Nichols CG (2006) KATP channels as molecular sensors of cellular metabolism. *Nature* **440:**470–476.
Nichols CG and Lederer WJ (1991) Adenosine triphosphate-sensitive potassium channels in the cardiovascular system. *Am J Physiol* **261:**H1675–H1686.
Noujaim SF, Stuckey JA, Ponce-Balbuena D, Ferrer-Villada T, López-Izquierdo A, Pandit S, Calvo CJ, Grzeda KR, Berenfeld O, Chapula JA, et al. (2010) Specific residues of the cytoplasmic domains of cardiac inward rectifier potassium channels are effective antifibrillatory targets. *FASEB J* **24:**4302–4312.
Noujaim SF, Stuckey JA, Ponce-Balbuena D, Ferrer-Villada T, López-Izquierdo A, Pandit SV, Sánchez-Chapula JA, and Jalife J (2011) Structural bases for the different anti-fibrillatory effects of chloroquine and quinidine. *Cardiovasc Res* **89:**862–869.
Pandit SV, Kaur K, Zlochiver S, Noujaim SF, Furspan P, Mironov S, Shibayama J, Anumonwo J, and Jalife J (2011) Left-to-right ventricular differences in I(KATP) underlie epicardial repolarization gradient during global ischemia. *Heart Rhythm* **8:**1732–1739.
Ponce-Balbuena D, López-Izquierdo A, Ferrer T, Rodríguez-Menchaca AA, Aréchiga-Figueroa IA, and Sánchez-Chapula JA (2009) Tamoxifen inhibits inward rectifier K^+ 2.x family of inward rectifier channels by interfering with phosphatidylinositol 4,5-bisphosphate-channel interactions. *J Pharmacol Exp Ther* **331:**563–573.
Ponce-Balbuena D, Moreno-Galindo EG, López-Izquierdo A, Ferrer T, and Sánchez-Chapula JA (2010) Tamoxifen inhibits cardiac ATP-sensitive and acetylcholine-activated K^+ currents in part by interfering with phosphatidylinositol 4,5-bisphosphate-channel interaction. *J Pharmacol Sci* **113:**66–75.

Ribalet B, John SA, Xie LH, and Weiss JN (2006) ATP-sensitive K+ channels: regulation of bursting by the sulphonylurea receptor, PIP2 and regions of Kir6.2. *J Physiol* **571:**303–317.

Rodríguez-Menchaca AA, Navarro-Polanco RA, Ferrer-Villada T, Rupp J, Sachse FB, Tristani-Firouzi M, and Sánchez-Chapula JA (2008) The molecular basis of chloroquine block of the inward rectifier Kir2.1 channel. *Proc Natl Acad Sci USA* **105:**1364–1368.

Sánchez-Chapula JA, Salinas-Stefanon E, Torres-Jácome J, Benavides-Haro DE, and Navarro-Polanco RA (2001) Blockade of currents by the antimalarial drug chloroquine in feline ventricular myocytes. *J Pharmacol Exp Ther* **297:**437–445.

Schulze D, Krauter T, Fritzenschaft H, Soom M, and Baukrowitz T (2003) Phosphatidylinositol 4,5-bisphosphate (PIP2) modulation of ATP and pH sensitivity in Kir channels. A tale of an active and a silent PIP2 site in the N terminus. *J Biol Chem* **278:**10500–10505.

Seeman P (1972) The membrane actions of anesthetics and tranquilizers. *Pharmacol Rev* **24:**583–655.

Shyng S, Ferrigni T, and Nichols CG (1997) Control of rectification and gating of cloned KATP channels by the Kir6.2 subunit. *J Gen Physiol* **110:**141–153.

Shyng SL, Cukras CA, Harwood J, and Nichols CG (2000) Structural determinants of PIP_2 regulation of inward rectifier K(ATP) channels. *J Gen Physiol* **116:**599–608.

Tamargo J, Caballero R, Gómez R, Valenzuela C, and Delpón E (2004) Pharmacology of cardiac potassium channels. *Cardiovasc Res* **62:**9–33.

Trapp S, Proks P, Tucker SJ, and Ashcroft FM (1998) Molecular analysis of ATP-sensitive K channel gating and implications for channel inhibition by ATP. *J Gen Physiol* **112:**333–349.

Varró A, Biliczki P, Iost N, Virág L, Hála O, Kovács P, Mátyus P, and Papp JG (2004) Theoretical possibilities for the development of novel antiarrhythmic drugs. *Curr Med Chem* **11:**1–11.

Whorton MR and MacKinnon R (2011) Crystal structure of the mammalian GIRK2 K+ channel and gating regulation by G proteins, PIP2, and sodium. *Cell* **147:**199–208.

Woodhull AM (1973) Ionic blockage of sodium channels in nerve. *J Gen Physiol* **61:**687–708.

Zhou W, Arrabit C, Choe S, and Slesinger PA (2001) Mechanism underlying bupivacaine inhibition of G protein-gated inwardly rectifying K^+ channels. *Proc Natl Acad Sci USA* **98:**6482–6487.

Address correspondence to: Dr. José A. Sánchez-Chapula, Unidad de Investigación "Carlos Méndez" del Centro Universitario de Investigaciones Biomédicas de la Universidad de Colima, Av 25 de Julio 965 Col. Villas San Sebastián, Colima, Col. México, CP 28045. E-mail: sancheza@ucol.mx